Molecules and Cells

LncRNA H19/miR-29b-3p/PGRN Axis Promoted Epithelial-Mesenchymal Transition of Colorectal Cancer Cells by Acting on Wnt Signaling

Dayong Ding[1], Changfeng Li[2,*], Tiancheng Zhao[2], Dandan Li[2], Lei Yang[2], and Bin Zhang[2]

[1]Department of Gastrointestinal Surgery, China-Japan Union Hospital of Jilin University, Changchun, Jilin 130033, P.R. China, [2]Department of Endoscopy Center, China-Japan Union Hospital of Jilin University, Changchun, Jilin 130033, P.R. China
*Correspondence: Med_lichangfenghj@yeah.net
http://dx.doi.org/10.14348/molcells.2018.2258
www.molcells.org

This investigation was aimed at working out the combined role of lncRNA H19, miR-29b and Wnt signaling in the development of colorectal cancer (CRC). In the aggregate, 185 CRC tissues and corresponding para-carcinoma tissues were gathered. The human CRC cell lines (i.e. HT29, HCT116, SW480 and SW620) and normal colorectal mucosa cell line (NCM460) were also purchased. Si-H19, si-NC, miR-29b-3p mimics, miR-29b-3p inhibitor, si-PGRN and negative control (NC) were, respectively, transfected into the CRC cells. Luciferase reporter plasmids were prepared to evaluate the transduction activity of Wnt/β-catenin signaling pathway, and dual-luciferase reporter gene assay was arranged to confirm the targeted relationship between H19 and miR-29b-3p, as well as between miR-29b-3p and PGRN. Finally, the proliferative and invasive capacities of CRC cells were appraised through transwell, MTT and scratch assays. As a result, overexpressed H19 and down-expressed miR-29b-3p displayed close associations with the CRC patients' poor prognosis ($P < 0.05$). Besides, transfection with si-H19, miR-29b-3p mimic or si-PGRN were correlated with elevated E-cadherin expression, decreased snail and vimentin expressions, as well as less-motivated cell proliferation and cell metastasis ($P < 0.05$). Moreover, H19 was verified to directly target miR-29b-3p based on the luciferase reporter gene assay ($P < 0.05$), and miR-29b-3p also bound to PGRN in a direct manner ($P < 0.05$). Finally, addition of LiCl (Wnt/β-catenin pathway activator) or XAV93920 (Wnt/β-catenin pathway inhibitor) would cause remarkably altered E-cadherin, c-Myc, vimentin and snail expressions, as well as significantly changed transcriptional activity of β-catenin/Tcf reporter plasmid ($P < 0.05$). In conclusion, the lncRNA H19/miR-29b-3p/PGRN/Wnt axis counted a great deal for seeking appropriate diagnostic biomarkers and treatment targets for CRC.

Keywords: colorectal cancer, EMT, lncRNA H19, miR-29b-3p, PGRN, Wnt signaling

INTRODUCTION

Colorectal cancer (CRC), the third most prevalent cancer worldwide, was responsible for 10% of all cancer-related mortality (Siegel et al., 2012). In spite of diverse diagnostic and therapeutic techniques, the five-year survival rate of CRC still remained low at 64.9% (Siegel et al., 2014). In fact, approximately 90% of CRC-relevant mortality could be chiefly attributed to distant metastasis, and epithelial-to-mesenchymal transition (EMT) counted a great deal within the metastatic course (Gupta and Massague, 2006). For instance, with initiation of EMT, the CRC masses would migrate to surrounding tissues or distant organs through blood and lymphatic vessels (Polyak and Weinberg, 2009; Thiery et al., 2009). Underlying this biological course, the involved factors included multiple transcriptional molecules, including

Received 16 October, 2017; revised 30 December, 2017; accepted 14 January, 2018; published online 10 May, 2018

eISSN: 0219-1032

transforming growth factor β (TGF-β), bone morphogenetic protein (BMP), Twist, Smads, snail and slug, and transcription-related pathways (e.g. Wnt/β-catenin, Hedgehog, and Notch signaling pathways) (Gonzalez and Medici, 2014; Liu et al., 2015).

LncRNAs, the non-coding RNAs characterized by a length of over 200 nt, could interact with distinct classes of RNAs (e.g. miRNAs) to influence various aspects of cellular homeostasis, including genomic stability, cell proliferation and cell migration. Certain lncRNAs have been identified as the potential biomarkers for CRC, for instance, evidences showed that elevated lncRNA H19 expression was strongly associated with the progression of CRC (Tsang et al., 2010; Xie et al., 2016). LncRNA H19 was a maternally expressed gene mapped to human chromosome 11, and one single nucleotide polymorphism (SNP) situated within it (i.e. rs2839698) was demonstrated to elevate susceptibility to CRC among a Chinese population (Gabory et al., 2010; Li et al., 2016; Thorvaldsen et al., 1998). Besides, H19 not only promoted malignant transformation of CRC through modifying miR-675 (Tsang et al., 2010), but also served as a positive regulator of EMT for CRC (Liang et al., 2015). Intriguingly, the functions of lncRNAs were usually mediated by regulation of microRNAs (miRNAs), which post-transcriptionally regulated gene expressions by binding to 3' untranslated region (UTR) of mRNAs (Shukla et al., 2011). For example, H19 negatively modifying tenogenic differentiation was achieved by direct target of miR-29b-3p and then suppression of TGF-β1 and COL1A1 expressions (Lu et al., 2017). Due to the strong correlation between miRNA expression profiles and cancer malignancies, certain miRNAs may be quite promising for diagnosing or predicting the prognosis of CRC, such as miR-195, miR-34a and miR-29b-3p (Hur et al., 2013; Liu et al., 2010; Poudyal et al., 2013; Yamakuchi et al., 2008; Ye et al., 2013; Yu et al., 2012). Thus, it was hypothesized that H19 possibly functioned on miR-29b-3p to modulate the presence and aggravation of CRC.

Besides, microRNA-29b could contribute to suppressed angiogenesis, invasion, and metastasis of hepatocellular carcinoma by targeting matrix metalloproteinase-2 (MMP-2) (Fang et al., 2011). Emerging evidences also suggested that the synthetic role of miR-29b and MMP-2 was essential for constraining migration of CRC cells (Poudyal et al., 2013). Moreover, miR-29b could negatively modulate the canonical Wnt signaling pathway, thereby reversing the epithelial to mesenchymal transition (EMT) process (Subramanian et al., 2014). Interestingly, since miR-29b-3p promoted apoptosis of chondrocytes via modifying progranulin (PGRN) (Chen et al., 2017), and PGRN acting on Wnt/β-catenin signaling was involved in the etiology of psoriasis (Tian et al., 2016), it was speculated that the interactive effects of miR-29b and Wnt signaling on EMT process could be mediated by PGRN. Of note, the particularized mechanisms concerning Wnt signaling and EMT development were dissimilar within varied cancers. For instance, inhibited EMT in gastric cancer was in part caused by VGLL4-mediated suppression of Wnt/β-catenin signaling, and EMT occurring in renal carcinoma was promoted by MUC1 (Gnemmi et al., 2014; Li et al., 2015). Nonetheless, the underlying mechanisms of Wnt signaling in modifying EMT process of CRC remained poorly understood.

In a nutshell, this investigation was purposed to explore whether H19 played a part in facilitating the EMT process of CRC through acting on the downstream miR-29b-3p and PGRN, and if Wnt signaling would be subject to the actions of H19, miR-29b-3p and PGRN in mediating this mechanism.

RESULT

Expressions of lncRNA H19 and miR-29b-3p within CRC cells and tissues

According to the TCGA Data Portal from starBASEv2.0, H19 expression within cancer tissues surpassed that within normal tissues ($P < 0.05$), and up-regulated H19 expression could be found within CRC tissues in comparison to normal tissues (Supplementary Fig. S1). Moreover, the expression of miR-29b-3p decreased apparently ($P < 0.05$) in the collected CRC tissues, when compared with adjacent normal tissues ($P < 0.05$) (Fig. 1A). Apart from that, H19 expression within CRC cell lines (i.e. HT29, HCT116, SW480 and SW620) picked up notably in comparison to normal colorectal mucosa

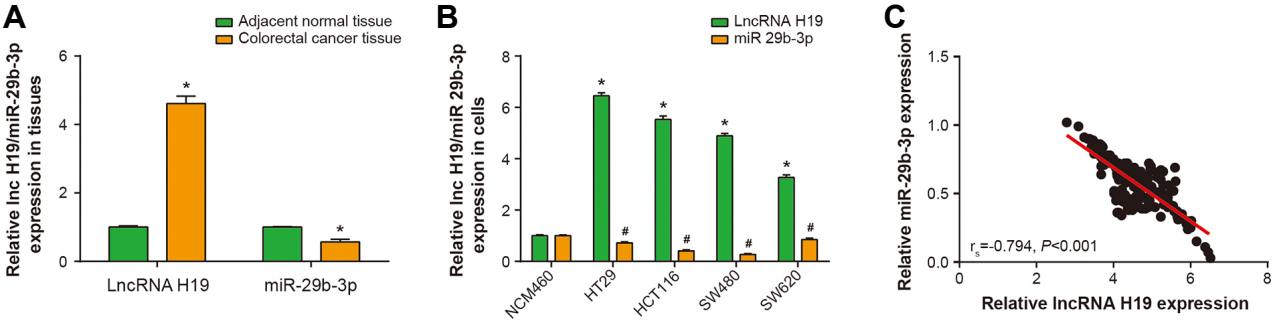

Fig. 1. The expression of lncRNA H19 and miR-29b-3p within colorectal cancer (CRC) tissues and cell lines. (A) LncRNA H19 and miR-29b-3p expressions were compared between CRC tissues and adjacent normal tissues. $*P < 0.05$ when compared with adjacent normal tissues. (B) LncRNA H19 and miR-29b-3p expression were compared among NCM460, HT29, HCT116, SW480 and SW620 cells. $*P < 0.05$ when compared with LncRNA H19 expression of NCM460 cell line; $^{\#}P < 0.05$ when compared with miR-29b-3p expression of NCM460 cell line. (C) LncRNA H19 expression was negatively correlated with miR-29b-3p expression within CRC tissues.

cell line (i.e. NCM460) ($P < 0.05$). However, miR-29b-3p expression within HT29, HCT116, SW480 and SW620 was significantly lower than that within NCM460 ($P < 0.05$) (Fig. 1B). Also a significantly negative correlation was exhibited between H19 expression and miR-29b-3p expression (r_s = -0.794, $P < 0.05$) (Fig. 1C).

The correlation between LncRNA H19/miR-29b-3p expressions and CRC patients' clinical features

The CRC patients were categorized into highly-expressed H19 group (H19 expression > median) and lowly-expressed H19 group (H19 expression ≤ median). The population was again divided into highly-expressed miR-29b-3p group (miR-29b-3p expression > median) and lowly-expressed miR-29b-3p group (miR-29b-3p expression ≤ median). The over-expressed H19 and under-expressed miR-29b-3p both exhibited tight linkages with CRC patients that were featured by poor differentiation, T3 + T4 stage and M1 distant metastasis ($P < 0.05$) (Table 1). However, scarcely any remarkable correlations were found between H19 or miR-29b-3p expressions and age, gender, tumor location and histology ($P > 0.05$).

Besides, the regression analysis demonstrated that high H19 expression, low miR-29b-3p expression, poor differentiation, T3 + T4 stage and M1 distant cell presented high correlations with poor prognosis of CRC patients ($P < 0.05$) (Table 2). Additionally, Kaplan Meier analysis displayed that the overall survival (OS) rate of patients with under-expressed H19 and over-expressed miR-29b-3p performed far better than that of ones with over-expressed H19 and under-expressed miR-29b-3p ($P < 0.05$) (Fig. 2).

H19 and miR-29b-3p regulated motility, EMT, invasion and migration of CRC cells

In order to figure out whether H19 and miR-29b-3p regulated migration and invasion of CRC cells through inducing EMT, we detected E-cadherin, Snail and Vimentin expressions within CRC cell lines (Figs. 3A and 3B). The expression level of E-cadherin hiked, and Snail and Vimentin expressions fell off visibly in the si-H19 group, when compared with si-NC group ($P < 0.05$). In addition, miR-29b-3p inhibitor constrained the expression of E-cadherin obviously, and increased the expressions of Vimentin and Snail clearly ($P < 0.05$).

Table 1. The relationship between lncRNA H19/miR 29b-3p expression and the colorectal cancer patients' clinical characteristics

Characteristics	LncRNA H19 expression			miR 29b-3p expression		
	Low	High	*P*	Low	High	*P*
N=185	60	125		114	71	
Age						
≤59	33	65		58	40	
>59	27	60	0.702	56	31	0.469
Sex						
Male	29	77		68	38	
Female	31	48	0.088	46	33	0.413
Smoking History						
Yes	14	21		18	17	
No	46	104	0.288	96	54	0.169
Tumor size						
≥ 5 cm	22	67		62	27	
< 5 cm	38	58	0.031	52	44	0.03
Tumor Differentiation Statue						
Poor Differentiation+Moderate Differentiation	20	71		65	26	
Well Differentiation	40	54	0.003	49	45	0.007
Lymphatic invasion						
Yes	36	45		39	42	
No	24	80	0.002	75	29	0.001
Tumor Depth Invasion						
pT3+pT4	24	74		69	29	
pT1+pT2	36	51	0.014	45	42	0.009
Histological Grade						
III	33	49		51	31	
I+II	27	76	0.043	63	40	0.886
TNM Stage						
III+IV	25	73		67	31	
0+I+II	35	52	0.033	47	40	0.045

Table 2. The correlation between characteristics and the colorectal cancer patients' overall survival

Characteristics	Univariate analysis			Multivariate analysis		
	Hazard Ratio	95% CI	*P*value	Hazard Ratio	95% CI	*P*value
LncRNAH19 expression						
High vs. Low	3.398	2.14-5.41	<0.001	3.506	2.09-5.85	<0.001
miR 29b-3p expression						
High vs. Low	0.288	0.19-0.44	<0.001	0.231	0.14-0.39	<0.001
Age						
≤59 vs. >59	0.93	0.65-1.33	0.688	1.003	0.69-1.47	0.989
Sex						
Male vs. Female	0.987	0.69-1.41	0.945	1.129	0.77-1.65	0.531
Smoking History						
No vs. Yes	0.994	0.63-1.56	0.979	0.609	0.38-0.98	0.04
Tumor size						
< 5 cm vs. ≥ 5cm	0.597	0.42-0.85	0.005	0.844	0.59-1.22	0.361
Tumor Differentiation Statue						
Well Differentiation vs. Poor Differentiation+Moderate Differentiation	0.39	0.27-0.56	<0.001	0.514	0.35-0.75	0.001
Lymphatic invasion						
No vs. Yes	1.307	0.90-1.89	0.157	0.5	0.31-0.82	0.006
Tumor Depth Invasion						
pT1+pT2 vs. pT3+pT4	0.52	0.36-0.75	<0.001	0.669	0.46-0.97	0.034
Histological Grade						
I+II vs. III	0.836	0.59-1.19	0.323	0.642	0.43-0.95	0.026
TNM Stage						
0+I+II vs. III+IV	0.461	0.32-0.67	<0.001	0.542	0.37-0.80	0.002

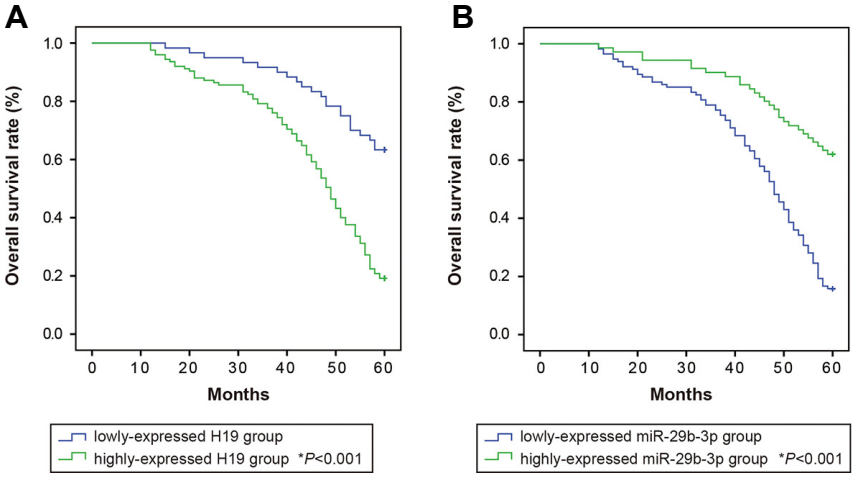

Fig. 2. The Kaplan-Meier curve was established for CRC patients carrying differentially expressed LncRNA H19 (A) and miR-29b-3p (B).

Meanwhile, the MTT results went as that the cell viability of si-H19 group and miR-29b-3p mimic group declined evidently in comparison to the control group (P < 0.05). Nonetheless, the cell viability was elevated apparently in the miR-29b-3p inhibitor group (*P* < 0.05) (Figs. 3C and 3D). Furthermore, the Transwell assay results indicated that the number of trans-membrane cells in the si-H19 group or in the miR-29b-3p mimic group was reduced remarkably (*P* < 0.05), whereas the number of trans-membrane cells in the miR-29b-3p inhibitor group picked up enormously than that in the control group (*P* < 0.05) (Fig. 4). Ultimately, it was witnessed from the scratch assay that the migratory ability of CRC cells in the si-H19 and miR-29b-3p mimic groups appeared much lower than the control group (*P* < 0.05), nonetheless, the migration ability of miR-29b-3p inhibitor group appeared much higher (P < 0.05) (Fig. 5).

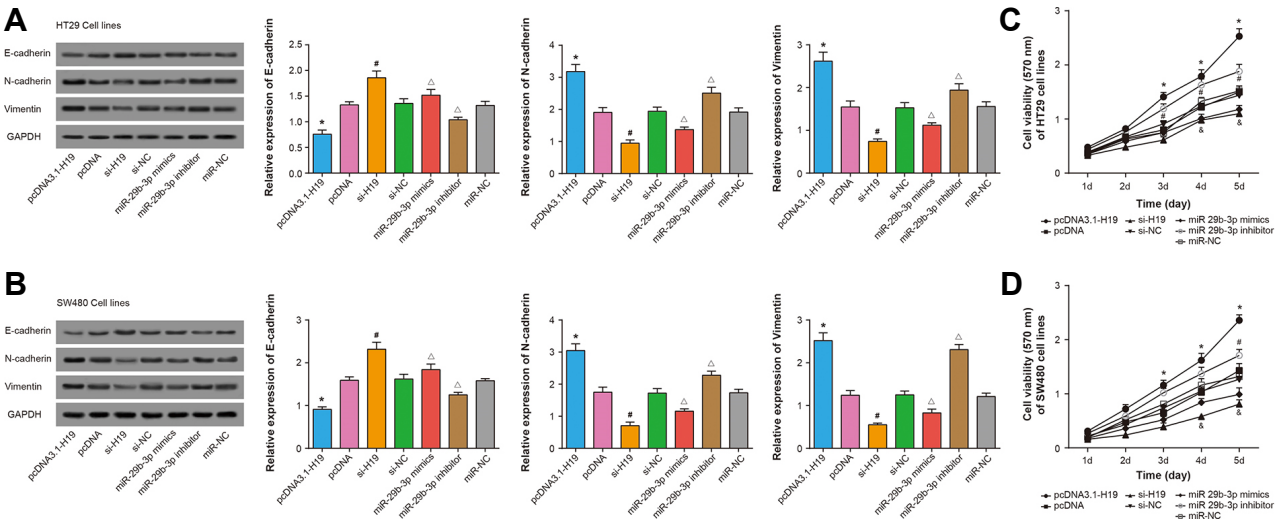

Fig. 3. The E-cadherin, N-cadherin and vimentin expression within HT29 (A) and SW480 (B) cell lines, along with the viability of HT29 (C) and SW480 (D) cell lines among pcDNA3.1-H19, pcDNA, si-H19, si-NC, miR-29b-3p mimic, miR-29b-3p inhibitor and miR-NC groups. $*P < 0.05$ when compared with pcDNA; $\Delta P < 0.05$ when compared with si-NC; $^{\#}P < 0.05$ when compared with miR-NC.

H19 targeted miR-29b-3p to inhibit its expression

The targeting sites for H19 and miR-29b-3p were predicted through Starbase 2.0 software (http://starbase.sysu.edu.cn/seedTargetInfo.php?type=lncRNA&database=hg19&name=hsa-miR-29b-3p&geneName=H19&autoId=1024&orgTable=mirLncRNAInteractionsAll) (Fig. 6A). In addition, the luciferase activity of H19 Wt+miR-29b-3p mimics group declined more notably than that of control group ($P < 0.05$). Nevertheless, the luciferase activity of H19 Mut + miR-29b-3p mimics group was similar to that of psiCHECK2 group or control group ($P > 0.05$) (Figs. 6B and 6C). Moreover, qRT-PCR results demonstrated that addition of si-H19 could evidently increase the expression of miR-29b-3p ($P < 0.05$), but there was little change of H19 expression when miR-29b-3p expression was modified ($P > 0.05$) (Figs. 6D and 6E).

MiR-29b-3p regulated Wnt/β-catenin signaling by targeting downstream PGRN

Silencing of miR-29b-3p fostered highly-expressed PGRN ($P < 0.05$), and the up-regulated miR-29b-3p expressions led to lowly-expressed PGRN ($P < 0.05$) (Fig. 6F). Besides, to verify whether miR-29b-3p directly interacted with PGRN to play a role, luciferase reporter assay was conducted. It could be derived from Fig. 6G that miR-29b-3p mimic+PGRN group contributed to a remarkably lower luciferase expression than NC group ($P < 0.05$). Conversely, co-transfection of mutated miR-29b-3p with PGRN was no different from the NC group ($P < 0.05$), suggesting that miR-29b-3p targeted PGRN to reduce its expression.

Moreover, the transcriptional activity of β-catenin/Tcf reporter plasmid within miR-29b-3p group and si-PGRN group was below that of NC group ($P < 0.05$), whereas H19 group was detected with an incremental gap concerning the plasmid transcriptional activity of β-catenin/Tcf reporter ($P < 0.05$) (Figs. 6H and 6I). Similarly, the expressions of β-catenin, c-Myc and cyclin D1 were inhibited within miR-29b-3p and si-PGRN groups, yet they all ascended evidently within H19 group ($P < 0.05$) (Fig. 7).

The H19/miR-29b-3p/PGRN axis modulated EMT of NSCLC cells via Wnt/β-catenin signaling

The expressions of EMT-marker proteins were observed after addition of 20 mmol/L LiCl (i.e. Wnt/β-catenin pathway activator) or 10 μmol/LXAV93920 (i.e. Wnt/Catenin pathway inhibitor) (Fig. 8). The miR-145-5p+XAV93920 group was associated with notably increased E-cadherin expression, yet markedly dropped expressions of c-Myc, vimentin and Snail, when compared with the miR-29b-3p group ($P < 0.05$). However, in comparison to H19 group, greatly reduced E-cadherin expression, accompanied with evidently elevated c-Myc, vimentin and Snail expressions were observed in the H19+XAV93920 and PGRN+XAV93920 groups ($P < 0.05$). Moreover, miR-29b-3p+LiCl group possessed far lower E-cadherin expression, along with higher c-Myc, vimentin or snail expressions than miR-29b-3p group ($P < 0.05$). Correspondingly, the E-cadherin expressions of H19+LiCl and PGRN+XAV93920 groups were both on the rise in comparison to H19 group, while their c-Myc, vimentin and Snail expressions lessened terribly ($P < 0.05$).

DISCUSSION

Generally speaking, the screening methods for CRC were limited, and the techniques were tough to be popularized. Hence, multiple CRC patients were not diagnosed until their lymphatic or distant metastasis was observed, which obviously affected the CRC population's prognosis. In addition, owing to the heterogeneity of CRC, specific therapeutic schedules should be prepared for diverse patients with different CRC degrees, of distinct onset ages and with discrepant

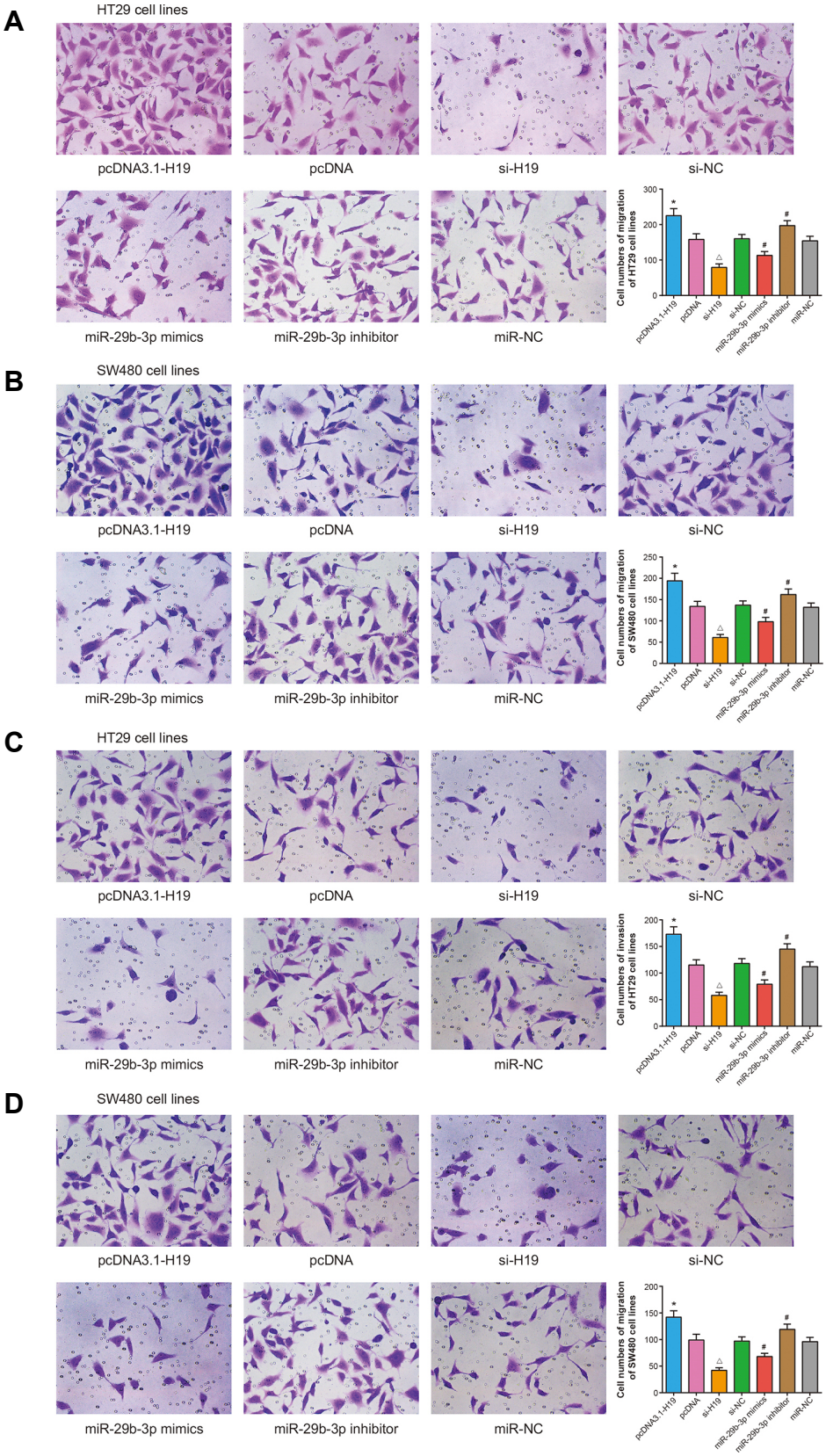

Fig. 4. The migratory (A-B) and invasive (C-D) abilities of SW480 and HT29 cell lines were determined with transwell assay among pcDNA3.1-H19, pcDNA, si-H19, si-NC, miR-29b-3p mimic, miR-29b-3p inhibitor and miR-NC groups. $*P < 0.05$ when compared with pcDNA; $\Delta P < 0.05$ when compared with si-NC; $^{\#}P < 0.05$ when compared with miR-NC.

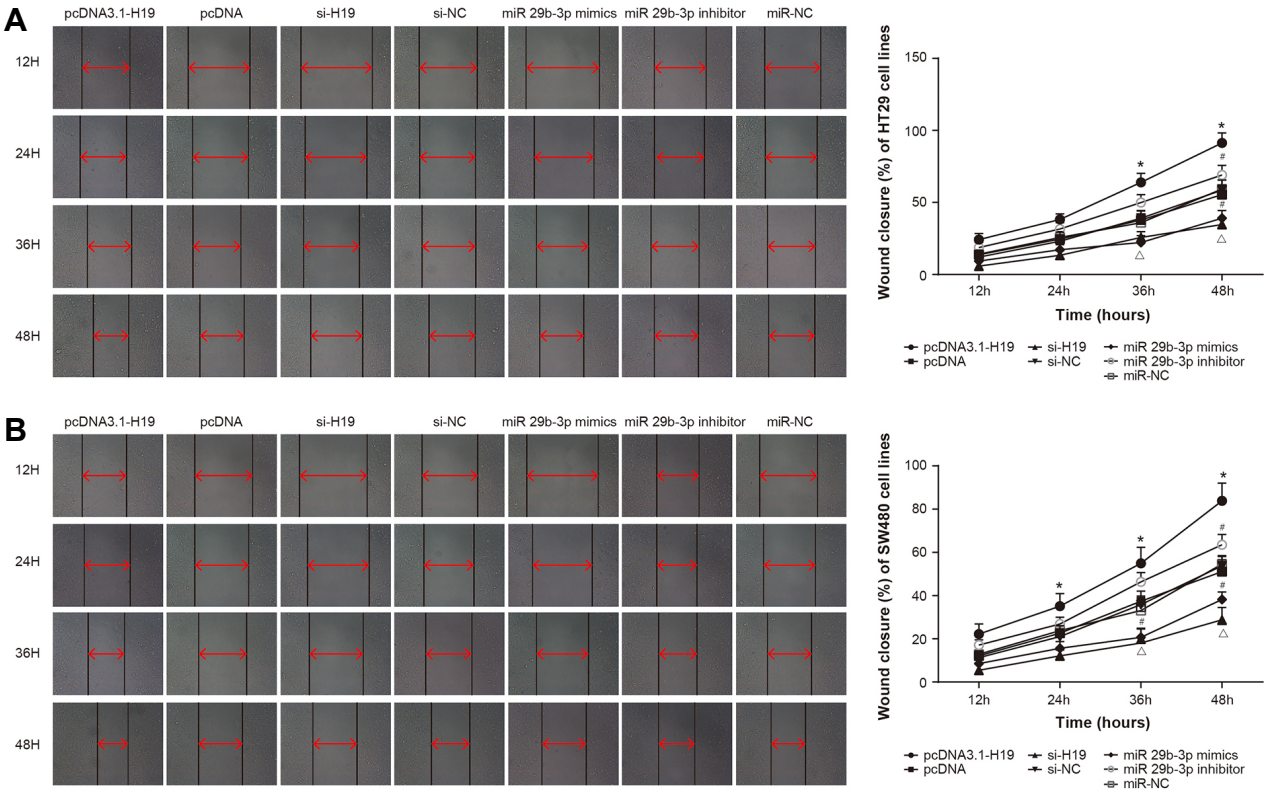

Fig. 5. The wound healing consequence of SW480 (A) and HT29 (B) cell lines were drawn at the time points of 12 h, 24 h, 36 h and 48 h, when groups of pcDNA3.1-H19, pcDNA, si-H19, si-NC, miR-29b-3p mimic, miR-29b-3p inhibitor and miR-NC were considered. $*P < 0.05$ when compared with pcDNA; $\Delta P < 0.05$ when compared with si-NC; $^{\#}P < 0.05$ when compared with miR-NC.

living habits. Furthermore, the incidence of drug-resistance for molecular-targeted therapies was also commonplace among the CRC population. Hence, seeking biomarkers for diagnosis of early-stage CRC, and uncovering novel molecular mechanisms for CRC were vital to improving the prognosis of CRC patients (Hardiman et al., 2016; Tsuji et al., 2009; Zhai et al., 2017).

It was noteworthy that lncRNAs could influence co-biology via modulation of miRNAs and related genes, and they also participated in such processes as chromosome remodeling, transcriptional control and RNA degradation. Besides, tissue specificity enabled the diagnostic sensitivity of lncRNAs to be higher than that of protein-coding RNAs and protein biomarkers (Slaby, 2016). Thus, it was insinuated that lncRNAs were well-equipped as the biomarker for cancers (e.g. CRC). Up to date, lncRNAs H19, MALAT1, CCAT1 and HOTAIR have been broadly recognized to facilitate the onset and development of CRC (Han et al., 2014; Ling et al., 2013; Slaby, 2016; Xue et al., 2015). Consistent with the previous studies, this study also believed that up-regulation of H19 expression was accompanied with the advent of cell metastasis and EMT (Fig. 3), which was specifically manifested as inhibited E-cadherin expression, elevated α-SMA expression and transition from epithelial cytokeratin to mesenchymal vimentin (Gillard et al., 2015). Once the above alterations were observed, worsening of CRC was probable to be initiated.

Furthermore, it was drawn that miR-29 was the targeted molecule of H19, and their synthetic effects also mediated CRC progression (Fig. 6). Virtually, miR-29b was obtained from human HeLa cells by direct cloning, and then miR-29a and miR-29c were successively gained (Dostie et al., 2003; Lagos-Quintana et al., 2001; 2002). Though the three subtypes of miR-29 shared the same sequence, miR-29b possessed an AGUGUU sequence in its 3'-end that was responsible for nuclear localization (Hwang et al., 2007). It was demonstrated that miR-29a/b/c positively regulated EMT within pancreatic cancer via holding up carcinoembryonic antigen (CEA)-related cell adhesion molecule-6 (CAM-6) expressions (Chen et al., 2013). Within breast cancer cells, miR-29 also hindered TGF-β-induced transition from hepatoma cell phenotype to mesenchymal cell phenotype through suppressing DNMT3B and DNMT1 expressions (Kogure et al., 2014). Moreover, miR-29 could down-regulate inhibitor of differentiation/DNA binding-1 (Id-1) expression within ovarian cancer cells, which was conducive to the TGF-β-causing occurrence of EMT (Teng et al., 2014). To sum up, miR-29 was of significance in blocking EMT risk, yet relevant mechanisms still demanded in-depth exploration.

Also, this study confirmed that miR-29b-3p might directly target PGRN to alter the downstream Wnt signaling, which modulated EMT process significantly (Figs. 7 and 8). Virtually,

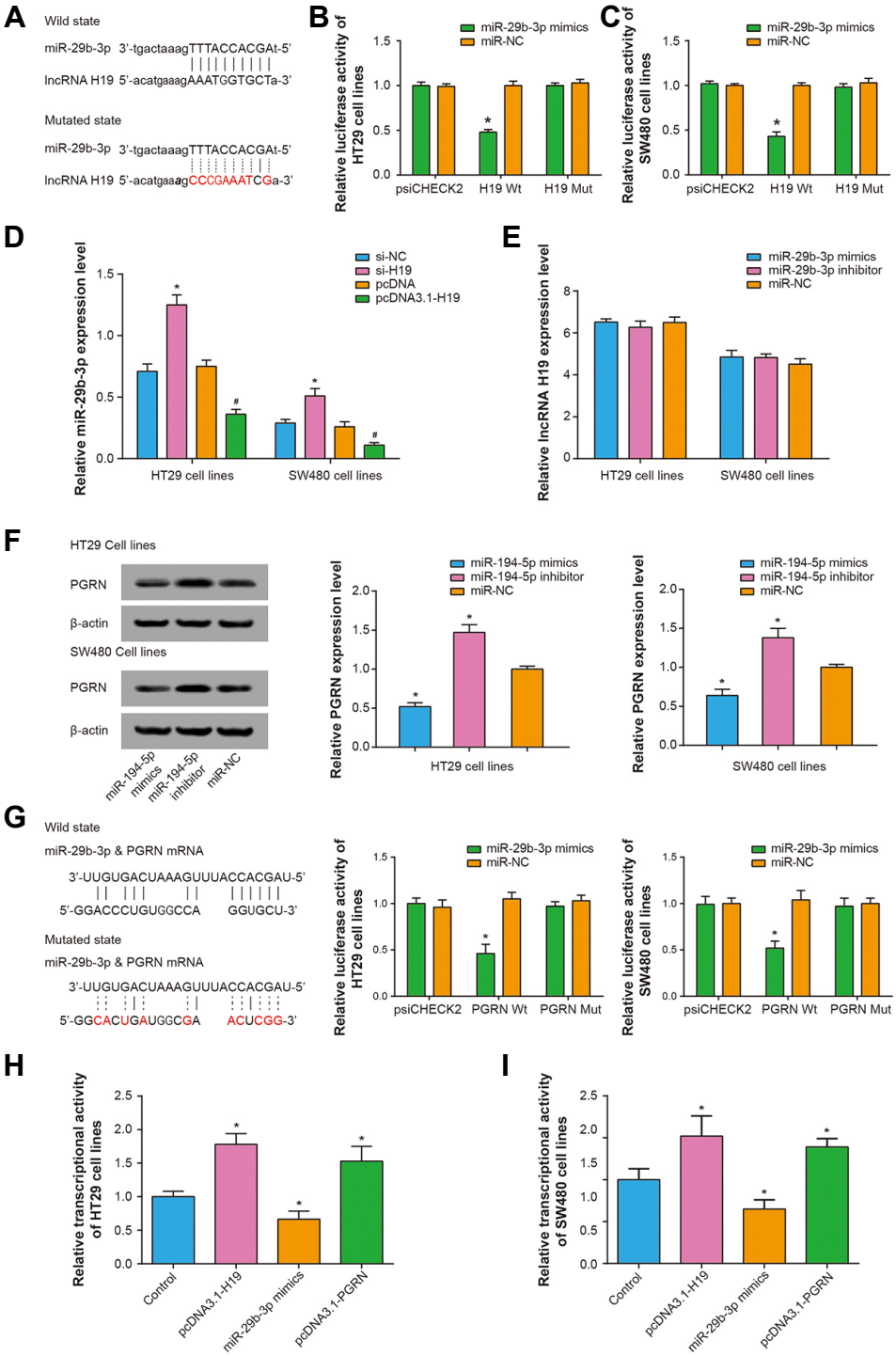

Fig. 6. The relationship between lncRNA H19 and miR-29b-3p, as well as between miR-29b-3p and PGRN. (A) LncRNA H19 was targeted by miR-29b-3p. (B-C) The luciferase activities of miR-29b-3p mimic+H19Wt and miR-29b-3p mimic+H19Mut were compared, respectively, within SW480 and HT29 cell lines. $*P < 0.05$ when compared with miR-NC. (D) The effect of pcDNA3.1-H19 on miR-29b-3p expression was determined within both SW480 and HT29 cell lines. $*P < 0.05$ when compared with si-NC; $^{\#}P < 0.05$ when compared with pcDNA. (E) The effects of miR-29b-3p inhibitor/mimic on H19 expression were detected within both SW480 and HT29 cell lines. (F) The effects of miR-194-5p mimic and miR-194-5p inhibitor on PGRN expression were assessed within both SW480 and HT29 cell lines. $*P < 0.05$ when compared with miR-NC. (G) MiR-29b-3p was targeted by PGRN, and the luciferase activities of miR-29b-3p mimic+ PGRN Wt and miR-29b-3p mimic+ PGRN Mut were compared within SW480 and HT29 cell lines. $*P < 0.05$ when compared with miR-NC. (H-I) The transcriptional activities of HT29 and SW480 cell lines were compared regarding control, pcDNA3.1-H19, miR-29b-3p mimics and pcDNA3.1-PGRN groups. $*P < 0.05$ when compared with control.

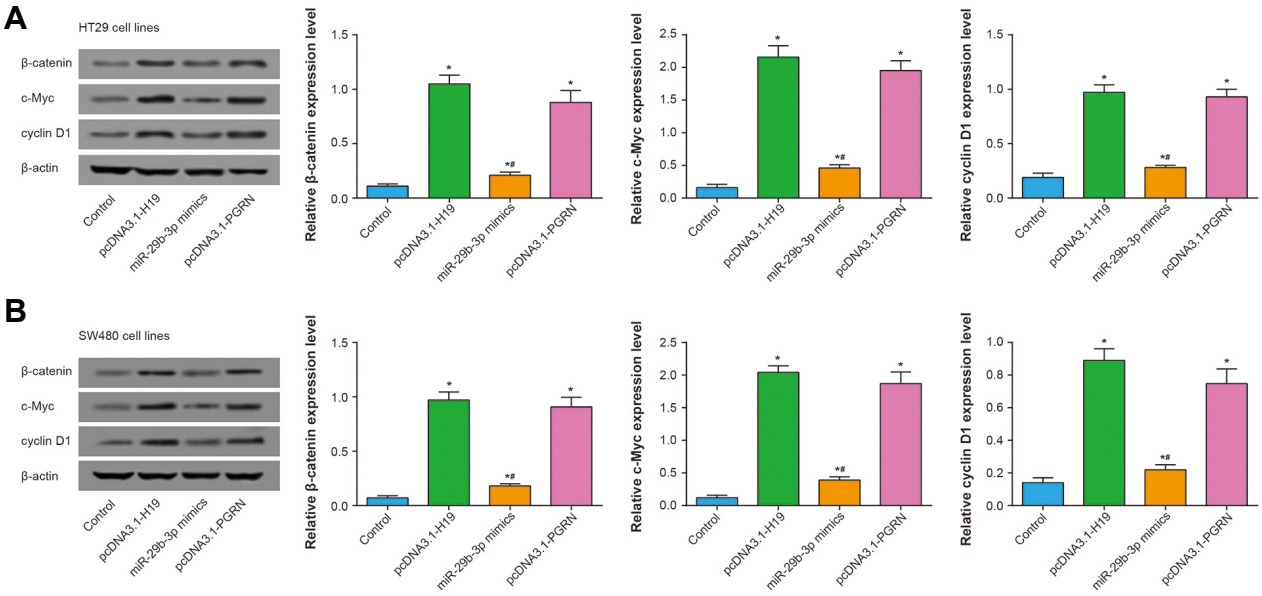

Fig. 7. The β-catenin, c-Myc and cyclin D1 expressions within and HT29 (A) and SW480 (B) cell lines were compared to the groups of control, pcDNA3.1-H19, miR-29b-3p mimics and pcDNA3.1-PGRN. $*P < 0.05$ when compared with control; $^{\#}P < 0.05$ when compared with pcDNA3.1-PGRN.

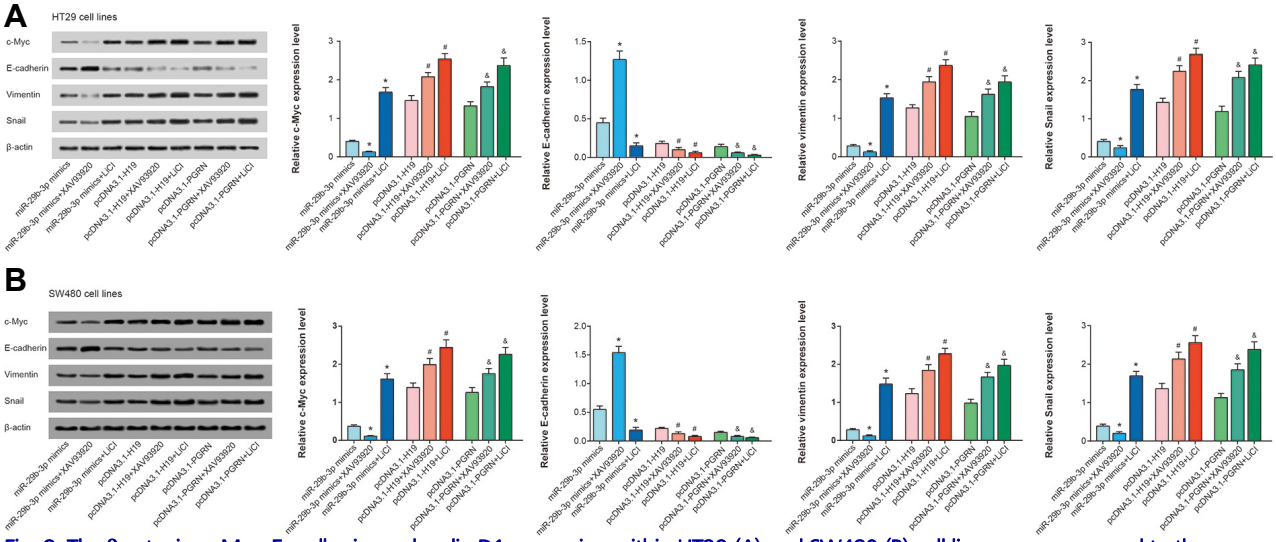

Fig. 8. The β-catenin, c-Myc, E-cadherin, and cyclin D1 expression within HT29 (A) and SW480 (B) cell lines were compared to the groups of miR-29b-3p mimics, miR-29b-3p mimics+XAV93920, miR-29b-3p mimics+LiCl, pcDNA3.1-H19, pcDNA3.1-H19+XAV93920, pcDNA3.1-H19+LiCl, pcDNA3.1-PGRN, pcDNA3.1-PGRN+XAV93920 and pcDNA3.1-PGRN +LiCl. $*P < 0.05$ when compared with miR-29b-3p mimics; $^{\#}P < 0.05$ when compared with pcDNA3.1-H19; $^{\&}P < 0.05$ when compared with pcDNA3.1-PGRN.

PGRN has been investigated in its association with EMT of epithelial ovarian cancer (EOC) cells, emphasizing its significance in modulating the pathogenesis of cancer cells' proliferation and invasion (Dong et al., 2016). Moreover, the functioning of classical Wnt signaling for EMT process has been deeply implicated in assorted publications. Specifically, when Wnt signaling was abnormally activated, β-catenin was separated from a degradation complex made up of axin/APC and GSK-3β (Huang and He, 2008). After binding to TCF/LEF, β-catenin further regulated progression of cell cycles by modulating marker proteins of EMT, such as c-Myc and cyclin D1 (Katoh and Katoh, 2007; Zhou et al., 2015). More than that, interdiction of Wnt/β-catenin pathway was accompanied by inhibited cell proliferation, promoted cell apoptosis and boosted EMT within pancreatic cancer animal models (Heiser et al., 2006; 2008; Pasca di Magliano et al.,

2007; Zhang et al., 2013). On the contrary, activated Wnt/β-catenin pathway depressed E-cadherin expression of EMT within breast infiltrating ductal carcinoma tissues (Prasad et al., 2009). Furthermore, curbing Snail-induced EMT progression would largely hindered epidermal cell carcinoma cells' invasive and migratory abilities, which further proved that aggravated EMT usually went with largely enhanced cell invasion and cell migration (Oft et al., 1998). All in all, it could be established that miR-29-3b/PGRN/Wnt signaling participated in the pathogenesis of the EMT process of CRC.

Conclusively, H19/miR-29-3b/PGRN/Wnt signaling was likely to stimulate the onset of EMT within CRC, which could greatly aid in exploring the diagnostic biomarkers and treatment targets for CRC.

MATERIALS AND METHODS

Collection of CRC tissues

One hundred and eighty-five pairs of CRC tissue samples and non-tumor normal tissues were taken from the general surgery of China-Japan Union Hospital of Jilin University, and the time span stretched from Dec. 2015 to Sep. 2016. All the patients were pathologically diagnosed as primary CRC, and they did not receive radiotherapy or chemotherapy before the surgery. The patients were averagely followed up for five years, and they have signed informed consents. This study was approved by China-Japan Union Hospital of Jilin University and the ethics committee of China-Japan Union Hospital of Jilin University.

Cell culture

Human CRC cell lines (i.e. HCT116, HT-29, SW620 and SW480) were purchased from cell inventory of Chinese Academy of Sciences (China), and were cultured with DMEM (Gibco). The fetus-sourced normal colorectal mucosa cell line (i.e. NCM460) was gained from American Type Culture Collection (ATCC), and was cultured within RPMI 1640 medium (Gibco). All the media were added with 10% fetal bovine serum (FBS), 100 U/ml penicillin and 100 μg/ml streptomycin. Then the cells were cultivated in 5% CO_2 at 37℃, and they would be digested with 0.25% trypsin at the phase of logarithmic growth.

Cell Transfection

Genepharma Inc. (China) accomplished the synthesis of miR-29b-3p mimics, miR-29b-3p inhibitors, negative control (NC), pcDNA3.1-H19, pcDNA3.1-PGRN, pcDNA3.1, H19 targeting siRNA (si-H19) and si-NC. The sequences of si-H19, miR-29b-3p mimic, miR-29b-3p inhibitor and si-NC were successively enlisted as: 1) 5'-CUUUCUGUCACAUUGACCACACCUG-3'; 2) 5'-UAGCACCAUUUGAAAUCAGUGUU-3'; 3) 5'-AACACUGAUUUCAAAUGGUGCUA-3'; 4) 5'-CACUGAUUUCAAAUGGUGCUAUU-3'.

Cell transfection was performed using Lipofectamine 2000 (Invitrogen) according to the manufacturer's instructions. In particular, the cells were cultured within the 12-well plate (Corning, USA), and 1 μg cDNA construct/20 pmol of RNA oligonucleotides and 1.5 μl of Lipofectamine 3000 were incubated within 25 μl Opti-MEM medium. After the two solutions were mixed and incubated at room temperature for 5 min, the mixture was added to the orifice plate for 3-hour incubation at 37℃. Subsequently, after 24-hour transfection within DMEM that contained 10% FBS, the medium was replaced with the normal growth medium.

RNA extraction and qRT-PCR

In reference to the specifications of the reverse transcription kit (Takara), the following reverse transcription system (10 μl) was added to the PCR tube: 5× reverse transcriptase M-MLV buffer (2.0 μl), 10 Mm dNTP mix (0.5 μl), random 6 mers (0.5 μl), ribonuclease inhibitor (0.25 μl), reverse transcriptase M-MLV (0.25 μl), RNA (1.0 μg) and RNasefree H_2O. The reaction procedures went as follows: 1) conduction of reverse transcription at 37℃ for 60 min; 2) inactivation of reverse transcriptase at 85℃ for 5 min; and 3) preservation at 4℃.

Furthermore, the PCR reaction system worked with primers (Supplementary Table 1), SYBR Green Mix (10 μl), sterile double distilled water (7.4 μl), sense primer (0.8 μl), antisense primer (0.8 μl) and cDNA template (1.0 μl), according to the instructions of SYBR Green Mix reagent. With U6 as the internal reference, the PCR reaction of miR-29b-3p occurred under the following steps: 1) pre-denaturation at 95℃ for 1 min; 2) denaturation with 40 cycles of 95℃ for 5 s and 60℃ for 30 s; and 3) termination at 95℃ for 15 min. For another, the reaction of H19 went through the steps as follows: 1) pre-denaturation at 95℃ for 1 min; 2) denaturation with 40 cycles of 95℃ for 15 s, 60℃ for 60 s and 72℃ for 45 s. GADPH served as the internal reference for H19. Finally, the ratio of gene expression in the experimental group and that in the control group was calculated according to the following formula: folds = $2^{-[Ct\ (target\ gene)\ -Ct\ (GAPDH)]\ Experimental\ group\ -\ [Ct\ (target\ gene)\ -Ct\ (GAPDH\ )]\ Control\ group}$.

MTT

Until the bottom of the orifice was filled with cell monolayer, 5 mg/ml MTT (20 μl) was added. After incubating the cells for 4 h, 150 μl dimethyl sulfoxide was supplemented to each well. The mixture was then shaken at low speed for 10 min, so that the crystals could be dissolved sufficiently. The OD_{490} absorbance values for the samples were measured with the enzyme-linked immunometric meter.

Transwell assay

During the invasive process, the upper chamber surface of the bottom membrane was diluted with 50 mg/L Matrigel (1:8). After digesting the cells and discarding the culture medium, the serum-free medium that contained bovine serum albumin was managed to adjust cell density to 4 × 10^8 cells/L. The lower chamber was added with 600 μl complete medium that contained 10% fetal bovine serum (FBS), and the medium in the lower chamber was removed about 24-48 h later. Then 90% ethanol solution (v/v) was supplemented for fixation at room temperature for 30 min, and 0.1% crystal violet solution was applied for staining at room temperature for 10 min after air-dry. Eventually the cells within the upper chamber were wiped away with a cotton swab, and the number of cells in the lower chamber was

examined within 5 randomly observed images. As for the migration experiment, the matrigel glue was not required, and the remaining experimental steps were consistent with the invasion assay.

Scratch assay

The cells at the logarithmic growth phase were seeded in the 6-well plates at the density of 5×10^5, and they were incubated in 5% CO_2 at 37℃ for 24 h. Until the cells spread across the bottom of the plate, a vertical scratching mark was made at the center of the well plate. The cells were then washed subtly with PBS for twice, and were cultured for another 24 h after removal of cell fragments. The migratory condition of the cells at the scratches was observed under an inverted microscope, and the status of cells was analyzed via Image J software.

Western blotting

The cell lysis solution was employed to lyse the cells, and proteins were collected. Then 5 × loading buffer was added and the mixture was boiled for 10 min. After conduction of sodium dodecyl sulfate-polyacrylamide gel electrophoresis (SDS-PAGE), polyvinylidene fluoride (PVDF) membranes were transferred under the 300 mA constant current for 60-90 min. Subsequently, 5% skimmed milk powder was used to seal the PVDF membrane for 2 h, and primary anti-bodies for PGRN (1:1000, Abcam), E-cadherin (1:800, Abcam), Vimentin (1:1000, Abcam), Snail (1:1000, Abcam), β-catenin (1:8000, Abcam), c-Myc (1:1000, Cell Signaling Technology) and Cyclin D1 (1:1000, Cell Signaling Technology) were added. After another overnight incubation at 4℃, cells were added with horse radish peroxidase (HRP)-conjugated secondary antibodies (1: 15,000, Jackson Immuno Research Inc). Finally, freshly-made ECL luminescent solution was added to analyze the gray values.

Luciferase reporter plasmid detected the transduction activity of Wnt/β-catenin signal pathway

The cells at the state of exponential growth were paved in the T25 culture flask. When cells attacked to the wall, about 3 μg TCF4/LEF reporter plasmids (pTOP-Luc) were transfected into the cells with lipofectamine 2000. Twelve hours later, cells were digested and re-planted into the 24-well plates. After 24 h, the cells were lysed, and the luciferase activity was measured according to the instructions of fluoresce in reporter kit (NEB Cor.). The concentration of total protein within the lysate was gauged via BCA protein quantitative kit (Shanghai Generay BiotechCo., Ltd.).

Dual luciferase assay

The H19 cDNAs and PGRN cDNAs that contained specific miR-29b-3p binding sites were amplified by aid of PCR, and were then cloned into the luciferase reporter gene (i.e. psiCHECK2). In this way, H19 Wt and PGRN Wt were successfully constructed. Moreover, the luciferase reporter gene H19 Mut and PGRN Mut that possessed mutated sequences within the miR-29b-3p binding site were constructed. The above plasmids and reporter gene carriers were synthesized by Shanghai Sango Corporation (China). Next, miR-29b-3p mimics and miR-NC were, respectively, transfected into HT29 and SW480 cells that have been transfected with H19 Wt, H19 Mut, PGRN Wt, PGRN Mut and psiCHECK2. After 6-hour transfection and 60-hour spitting, luciferase reporter assay (Promega, USA) was implemented for the lysed cells, and the fluorescence values of renilla plasmid were taken as the internal reference.

Statistical method

All the statistical analyses were performed via SPSS 20.0 software. To be concrete, χ^2 test was adopted for comparing enumeration data, and the quantitative data [(mean ± standard deviation (SD)] were compared using t test. It was believed as statistically meaningful when *P* value was less than 0.05.

Note: Supplementary information is available on the Molecules and Cells website (www.molcells.org).

ACKNOWLEDGMENTS

This study was supported by Jilin Province Industrial Innovation Special Fund Project (2016CO51).

REFERENCES

Chen, J., Li, Q., An, Y., Lv, N., Xue, X., Wei, J., Jiang, K., Wu, J., Gao, W., Qian, Z., et al. (2013). CEACAM6 induces epithelial-mesenchymal transition and mediates invasion and metastasis in pancreatic cancer. Int. J. Oncol. *43*, 877-885.

Chen, L., Li, Q., Wang, J., Jin, S., Zheng, H., Lin, J., He, F., Zhang, H., Ma, S., Mei, J., et al. (2017). MiR-29b-3p promotes chondrocyte apoptosis and facilitates the occurrence and development of osteoarthritis by targeting PGRN. J. Cell. Mol. Med. *21*, 3347-3359.

Dong, T., Yang, D., Li, R., Zhang, L., Zhao, H., Shen, Y., Zhang, X., Kong, B., and Wang, L. (2016). PGRN promotes migration and invasion of epithelial ovarian cancer cells through an epithelial mesenchymal transition program and the activation of cancer associated fibroblasts. Exp. Mol. Pathol. *100*, 17-25.

Dostie, J., Mourelatos, Z., Yang, M., Sharma, A., and Dreyfuss, G. (2003). Numerous microRNPs in neuronal cells containing novel microRNAs. RNA *9*, 180-186.

Fang, J.H., Zhou, H.C., Zeng, C., Yang, J., Liu, Y., Huang, X., Zhang, J.P., Guan, X.Y., and Zhuang, S.M. (2011). MicroRNA-29b suppresses tumor angiogenesis, invasion, and metastasis by regulating matrix metalloproteinase 2 expression. Hepatology *54*, 1729-1740.

Gabory, A., Jammes, H., and Dandolo, L. (2010). The H19 locus: role of an imprinted non-coding RNA in growth and development. BioEssays *32*, 473-480.

Gillard, G., Shafaq-Zadah, M., Nicolle, O., Damaj, R., Pecreaux, J., and Michaux, G. (2015). Control of E-cadherin apical localisation and morphogenesis by a SOAP-1/AP-1/clathrin pathway in C. elegans epidermal cells. Development *142*, 1684-1694.

Gnemmi, V., Bouillez, A., Gaudelot, K., Hemon, B., Ringot, B., Pottier, N., Glowacki, F., Villers, A., Vindrieux, D., Cauffiez, C., et al. (2014). MUC1 drives epithelial-mesenchymal transition in renal carcinoma through Wnt/beta-catenin pathway and interaction with SNAIL promoter. Cancer Lett. *346*, 225-236.

Gonzalez, D.M., and Medici, D. (2014). Signaling mechanisms of the epithelial-mesenchymal transition. Science Signal. *7*, re8.

Gupta, G.P., and Massague, J. (2006). Cancer metastasis: building a framework. Cell *127*, 679-695.

Han, J., Rong, L.F., Shi, C.B., Dong, X.G., Wang, J., Wang, B.L., Wen, H., and He, Z.Y. (2014). Screening of lymph nodes metastasis associated lncRNAs in colorectal cancer patients. World J. Gastroenterol. *20*, 8139-8150.

Hardiman, K.M., Ulintz, P.J., Kuick, R.D., Hovelson, D.H., Gates, C.M., Bhasi, A., Rodrigues Grant, A., Liu, J., Cani, A.K., Greenson, J.K., et al. (2016). Intra-tumor genetic heterogeneity in rectal cancer. Lab Invest. *96*, 4-15.

Heiser, P.W., Lau, J., Taketo, M.M., Herrera, P.L., and Hebrok, M. (2006). Stabilization of beta-catenin impacts pancreas growth. Development *133*, 2023-2032.

Heiser, P.W., Cano, D.A., Landsman, L., Kim, G.E., Kench, J.G., Klimstra, D.S., Taketo, M.M., Biankin, A.V., and Hebrok, M. (2008). Stabilization of beta-catenin induces pancreas tumor formation. Gastroenterology *135*, 1288-1300.

Huang, H., and He, X. (2008). Wnt/beta-catenin signaling: new (and old) players and new insights. Curr. Opin. Cell Biol. *20*, 119-125.

Hur, K., Toiyama, Y., Takahashi, M., Balaguer, F., Nagasaka, T., Koike, J., Hemmi, H., Koi, M., Boland, C.R., and Goel, A. (2013). MicroRNA-200c modulates epithelial-to-mesenchymal transition (EMT) in human colorectal cancer metastasis. Gut *62*, 1315-1326.

Hwang, H.W., Wentzel, E.A., and Mendell, J.T. (2007). A hexanucleotide element directs microRNA nuclear import. Science *315*, 97-100.

Katoh, M., and Katoh, M. (2007). WNT signaling pathway and stem cell signaling network. Clin. Cancer Res. *13*, 4042-4045.

Kogure, T., Kondo, Y., Kakazu, E., Ninomiya, M., Kimura, O., and Shimosegawa, T. (2014). Involvement of miRNA-29a in epigenetic regulation of transforming growth factor-beta-induced epithelial-mesenchymal transition in hepatocellular carcinoma. Hepatol. Res. *44*, 907-919.

Lagos-Quintana, M., Rauhut, R., Lendeckel, W., and Tuschl, T. (2001). Identification of novel genes coding for small expressed RNAs. Science *294*, 853-858.

Lagos-Quintana, M., Rauhut, R., Yalcin, A., Meyer, J., Lendeckel, W., and Tuschl, T. (2002). Identification of tissue-specific microRNAs from mouse. Curr. Biol. *12*, 735-739.

Li, H., Wang, Z., Zhang, W., Qian, K., Liao, G., Xu, W., and Zhang, S. (2015). VGLL4 inhibits EMT in part through suppressing Wnt/beta-catenin signaling pathway in gastric cancer. Med. Oncol. *32*, 83.

Li, S., Hua, Y., Jin, J., Wang, H., Du, M., Zhu, L., Chu, H., Zhang, Z., and Wang, M. (2016). Association of genetic variants in lncRNA H19 with risk of colorectal cancer in a Chinese population. Oncotarget *7*, 25470-25477.

Liang, W.C., Fu, W.M., Wong, C.W., Wang, Y., Wang, W.M., Hu, G.X., Zhang, L., Xiao, L.J., Wan, D.C., Zhang, J.F., et al. (2015). The lncRNA H19 promotes epithelial to mesenchymal transition by functioning as miRNA sponges in colorectal cancer. Oncotarget *6*, 22513-22525.

Ling, H., Spizzo, R., Atlasi, Y., Nicoloso, M., Shimizu, M., Redis, R.S., Nishida, N., Gafa, R., Song, J., Guo, Z., et al. (2013). CCAT2, a novel noncoding RNA mapping to 8q24, underlies metastatic progression and chromosomal instability in colon cancer. Genome Res. *23*, 1446-1461.

Liu, L., Chen, L., Xu, Y., Li, R., and Du, X. (2010). microRNA-195 promotes apoptosis and suppresses tumorigenicity of human colorectal cancer cells. Biochem. Biophys. Res. Commun. *400*, 236-240.

Liu, X., Yun, F., Shi, L., Li, Z.H., Luo, N.R., and Jia, Y.F. (2015). Roles of Signaling Pathways in the Epithelial-Mesenchymal Transition in Cancer. Asian Pac J Cancer Prev. *16*, 6201-6206.

Lu, Y.F., Liu, Y., Fu, W.M., Xu, J., Wang, B., Sun, Y.X., Wu, T.Y., Xu, L.L., Chan, K.M., Zhang, J.F., et al. (2017). Long noncoding RNA H19 accelerates tenogenic differentiation and promotes tendon healing through targeting miR-29b-3p and activating TGF-beta1 signaling. FASEB J. *31*, 954-964.

Oft, M., Heider, K.H., and Beug, H. (1998). TGFβ signaling is necessary for carcinoma cell invasiveness and metastasis. Curr. Biol. *8*, 1243-1252.

Pasca di Magliano, M., Biankin, A.V., Heiser, P.W., Cano, D.A., Gutierrez, P.J., Deramaudt, T., Segara, D., Dawson, A.C., Kench, J.G., Henshall, S.M., et al. (2007). Common activation of canonical Wnt signaling in pancreatic adenocarcinoma. PloS one *2*, e1155.

Polyak, K., and Weinberg, R.A. (2009). Transitions between epithelial and mesenchymal states: acquisition of malignant and stem cell traits. Nat. Rev. Cancer *9*, 265-273.

Poudyal, D., Cui, X., Le, P.M., Hofseth, A.B., Windust, A., Nagarkatti, M., Nagarkatti, P.S., Schetter, A.J., Harris, C.C., and Hofseth, L.J. (2013). A key role of microRNA-29b for the suppression of colon cancer cell migration by American ginseng. PloS one *8*, e75034.

Prasad, C.P., Rath, G., Mathur, S., Bhatnagar, D., Parshad, R., and Ralhan, R. (2009). Expression analysis of E-cadherin, Slug and GSK3beta in invasive ductal carcinoma of breast. BMC Cancer *9*, 325.

Shukla, G.C., Singh, J., and Barik, S. (2011). MicroRNAs: processing, maturation, target recognition and regulatory functions. Mol. Cell. Pharmacol. *3*, 83-92.

Siegel, R., Naishadham, D., and Jemal, A. (2012). Cancer statistics, 2012. CA Cancer J Clin. *62*, 10-29.

Siegel, R., Desantis, C., and Jemal, A. (2014). Colorectal cancer statistics, 2014. CA Cancer J. Clin. *64*, 104-117.

Slaby, O. (2016). Non-coding RNAs as biomarkers for colorectal cancer screening and early detection. Adv. Exp. Med. Biol. *937*, 153-170.

Subramanian, M., Rao, S.R., Thacker, P., Chatterjee, S., and Karunagaran, D. (2014). MiR-29b downregulates canonical Wnt signaling by suppressing coactivators of beta-catenin in human colorectal cancer cells. J. Cell. Biochem. *115*, 1974-1984.

Teng, Y., Zhao, L., Zhang, Y., Chen, W., and Li, X. (2014). Id-1, a protein repressed by miR-29b, facilitates the TGFbeta1-induced epithelial-mesenchymal transition in human ovarian cancer cells. Cell. Physiol. Biochem. *33*, 717-730.

Thiery, J.P., Acloque, H., Huang, R.Y., and Nieto, M.A. (2009). Epithelial-mesenchymal transitions in development and disease. Cell *139*, 871-890.

Thorvaldsen, J.L., Duran, K.L., and Bartolomei, M.S. (1998). Deletion of the H19 differentially methylated domain results in loss of imprinted expression of H19 and Igf2. Genes Dev. *12*, 3693-3702.

Tian, R., Li, Y., and Yao, X. (2016). PGRN suppresses inflammation and promotes autophagy in keratinocytes through the Wnt/beta-catenin signaling pathway. Inflammation *39*, 1387-1394.

Tsang, W.P., Ng, E.K., Ng, S.S., Jin, H., Yu, J., Sung, J.J., and Kwok, T.T. (2010). Oncofetal H19-derived miR-675 regulates tumor suppressor RB in human colorectal cancer. Carcinogenesis *31*, 350-358.

Tsuji, T., Ibaragi, S., and Hu, G.F. (2009). Epithelial-mesenchymal transition and cell cooperativity in metastasis. Cancer Res. *69*, 7135-7139.

Xie, X., Tang, B., Xiao, Y.F., Xie, R., Li, B.S., Dong, H., Zhou, J.Y., and Yang, S.M. (2016). Long non-coding RNAs in colorectal cancer.

Oncotarget *7*, 5226-5239.

Xue, Y., Ma, G., Gu, D., Zhu, L., Hua, Q., Du, M., Chu, H., Tong, N., Chen, J., Zhang, Z., et al. (2015). Genome-wide analysis of long noncoding RNA signature in human colorectal cancer. Gene *556*, 227-234.

Yamakuchi, M., Ferlito, M., and Lowenstein, C.J. (2008). miR-34a repression of SIRT1 regulates apoptosis. Proc. Natl. Acad. Sci. USA *105*, 13421-13426.

Ye, J., Wu, X., Wu, D., Wu, P., Ni, C., Zhang, Z., Chen, Z., Qiu, F., Xu, J., and Huang, J. (2013). miRNA-27b targets vascular endothelial growth factor C to inhibit tumor progression and angiogenesis in colorectal cancer. PloS one *8*, e60687.

Yu, Y., Kanwar, S.S., Patel, B.B., Oh, P.S., Nautiyal, J., Sarkar, F.H., and Majumdar, A.P. (2012). MicroRNA-21 induces stemness by downregulating transforming growth factor beta receptor 2 (TGFbetaR2) in colon cancer cells. Carcinogenesis *33*, 68-76.

Zhai, Z., Yu, X., Yang, B., Zhang, Y., Zhang, L., Li, X., and Sun, H. (2017). Colorectal cancer heterogeneity and targeted therapy: Clinical implications, challenges and solutions for treatment resistance. Semin. Cell Dev. Biol. *64*, 107-115.

Zhang, Y., Morris, J.P.t., Yan, W., Schofield, H.K., Gurney, A., Simeone, D.M., Millar, S.E., Hoey, T., Hebrok, M., and Pasca di Magliano, M. (2013). Canonical wnt signaling is required for pancreatic carcinogenesis. Cancer Res. *73*, 4909-4922.

Zhou, Y., Liang, C., Xue, F., Chen, W., Zhi, X., Feng, X., Bai, X., and Liang, T. (2015). Salinomycin decreases doxorubicin resistance in hepatocellular carcinoma cells by inhibiting the beta-catenin/TCF complex association via FOXO3a activation. Oncotarget *6*, 10350-10365.